Energy Conversion and Management: X 27 (2025) 101051

Contents lists available at ScienceDirect

Energy Conversion and Management: X

journal homepage: www.sciencedirect.com/journal/energy-conversion-and-management-x

Thermal assessment of Li-ion batteries incorporating phase change materials using a new 2D model

A. Afass [a,*], B. Lamrani [b], B. Lebrouhi [a], M.A. Tankari [c], M. Karkri [c], S. Landini [d], T. Kousksou [a]

[a] Université de Pau et des Pays de L'Adour, E2S UPPA, SIAME, Pau, France
[b] Mohammed V University in Rabat, Faculty of Sciences, MANAPSE Laboratory, 1014 RP Rabat, Morocco
[c] Université Paris Est Creteil, CERTES, F-94010 Creteil, France
[d] School of Engineering, Mathematics and Physics, University of East Anglia, Norwich NR4 7TJ, United Kingdom

ARTICLE INFO

Keywords:
Thermal model
Phase change material
Li-Ion batteries
New European Driving Cycle

ABSTRACT

This paper presents a novel physical model to analyse the energy efficiency of a thermal management system based on a phase change material (PCM) for Li-ion batteries including diffusion and irreversible phenomena such as entropy. Real-world battery performance was assessed using the New European Driving Cycle (NEDC), which includes four urban routes and one ultra-urban route. The model's accuracy was validated against experimental data, and an in-depth analysis of various parameters was conducted. The results show that the choice of PCM melting temperature range is pivotal in the battery thermal management system (BTMS) performance, with RT-28HC and RT-31 exhibiting superior thermal regulation during the three charge and discharge cycles. Although the thermal gradient within the pack is often negligible under different ambient conditions, higher ambient temperatures (40 °C) or high convective coefficients (60 W/m2K) increased thermal gradients. Simulations reveal that combining PCM and active cooling systems is required to reduce thermal gradients and maintain temperature uniformity, especially in extreme conditions and long operating times. This new model provides a cost-effective, agile alternative to computationally intensive methods for analysing dynamic thermal behaviour during long charge and discharge cycles.

1. Introduction

To achieve the carbon neutrality and net-zero carbon emissions goal by 2050, clean energy technologies must be developed and deployed swiftly. Energy efficiency, wind and solar power, hydropower and nuclear power, electric mobility, and electric vehicles (EVs) are emphasised as critical stepping stone on the way to net zero emissions in the IEA's report (Net Zero by 2050) [1–3]. Likewise, successful implementation of environmentally friendly EVs is considered one of the most important solutions to meet aforementioned worldwide target [3]. In this context, many countries have shown their willingness to address the retirement of fuel-powered cars in order to promote the development of EVs and plug-in hybrid electric vehicle (PHEVs) (e.g. In France, a blanket ban on the fuel vehicle sale by 2040; in the United Kingdom, a complete ban on the sale of traditional diesel-powered cars by 2030; in China, the target of banning the sale of conventional fuel cars by 2030, and so on) [4–6].

Despite the various benefits that EVs offer, their batteries necessitate constant thermal management to avoid potential catastrophic failure. There is a daily occurrence of several EV fires and explosions caused by thermal runaway, which has led to growing concerns regarding the safety of EV [7,8]. As reported by Sun *et al.* [9], some typical EV fire accidents have been recorded recently. This presents a challenge for firefighters with a significant environmental impact. Tesla's first aid guide states that in case of a battery fire, it may require up to 24 h and up to 8,000 gallons (30,283 L) of water to completely extinguish and cool down the fire. This poses a potential risk to users, passengers, and the citizens [10]. Academics and researchers are compelled to examine the causal variables that contribute to catastrophic failures. Among the several factors, battery degradation and ageing are some critical elements that impact the battery performance, life span, and safety [9,11]. However, battery degradation is a complex phenomenon involving several physical and chemical processes. Degradation is linked to several complex mechanisms resulting from a variety of factors (e.g. intrinsic and extrinsic) [12]. Intrinsic factors are divided into two groups:

* Corresponding author.
E-mail address: aafass@univ-pau.fr (A. Afass).

https://doi.org/10.1016/j.ecmx.2025.101051
Received 21 January 2025; Received in revised form 30 April 2025; Accepted 3 May 2025
Available online 12 May 2025

Nomenclature

Cp	Specific heat capacity [J kg^{-1} K^{-1}]
F	Faraday number
h	Convective heat transfer coefficient [W m^{-2} K^{-1}]
I	Electrical Current [A]
m	Mass [kg]
P_{gen}	Heat generation of battery [W]
R	Internal resistance [Ω]
$R_{b\text{-}p}$	Thermal resistance between battery and PCM [K/W]
$R_{p\text{-}ext}$	Thermal resistance between PCM and exterior [K/W]
S	Surface
ΔS	The entropy variation
T	Temperature [°C]

Greek letter

ρ	Density [kg m^{-3}]

Subscript

b	Battery
cd	Conductive
cv	Convective
ext	Exterior
pcm	Phase change materiel

Acronyms

BEVs	Battery Electric Vehicles
BMS	Battery Management System
BTMS	Battery thermal management system
CFD	Computational fluid dynamics
CNT	Carbon nanotubes
CV	Control volume
EG	Expanded graphite
EVs	Electric Vehicles
HP	Heat port
Li-ion	Lithium-ion
NEDC	New european driving cycle
NMC	Nickel manganese cobalt
PHEV	plug-in hybrid electric vehicle
SOC	State of charge
TMS	Thermal management system

material characteristics and production technologies. Extrinsic factors result from battery operating conditions such as charging at a high C-rate, high state of charge (SoC), low and high temperature. In this way, a snapshot of the degradation modes, aging mechanisms, as well as affected components in Li-ion batteries is given by Lin *et al.* (see Fig. 1) [11].

When examining these several degradation modes, it can be concluded that the battery temperature is responsible for most of the aging processes within both electrodes. According to [7], the battery temperature needs to be kept between 15 °C and 35 °C to enhance the performance of battery cells[13,14]. A temperature over 35 °C increase the secondary reactions inside the battery, resulting in a reduction in capacity and aging of the life span [15]. Temperatures below 15 °C, on the other hand, increase the internal resistance of the battery and alter the kinetics of the reaction, limiting discharge capacity and resulting in a significant reduction in battery life [15]. Furthermore, sub-zero temperatures can cause internal short circuits in some cases [16]. It is worth noting that non-uniform temperature distribution can cause inconsistencies in the electrochemical process, resulting in lower battery pack performance and durability. Consequently, lithium-ion cells

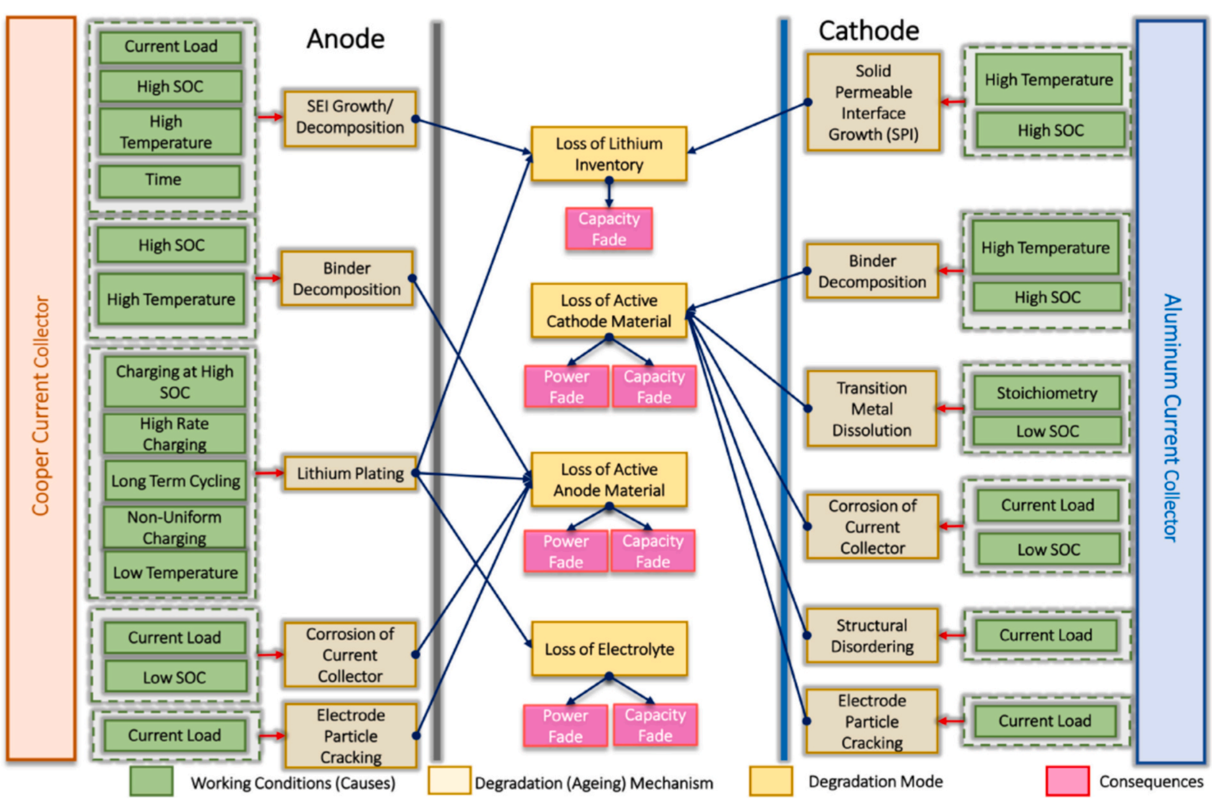

Fig. 1. Degradation modes, aging mechanisms and the affected components in Lithium-ion batteries [11].

require continuous thermal management to ensure sustained reliability and prevent catastrophic failures [17–20] by means of an effective battery thermal management system (BTMS) to control the battery temperature during charging and discharging cycles [21].

To address all these issues, numerous BTMS have been designed, tested, and experimentally studied [22–28]. These BTMS may be broken down into more specific categories according to their location (internal or external), transfer media (liquid, PCM or air) purpose (cooling or heating), and the source of energy (active or passive) [7,29–31]. Numerous studies in the literature thoroughly investigate these strategies from different points of view [28,32,33]. Among these methods, PCM-based BTMS stands out as an efficient way to cool batteries by dissipating their heat during solid-to-liquid phase change without draining auxiliary power [34]. The structural simplicity, high temperature control ability, low cost, stable chemical properties, and applicability are the main benefits of PCM-based BTMS [35–37]. However, thermal, physical, chemical kinetics, and economic viability must be considered while selecting the appropriate PCM [38]. Furthermore, PCM must have a melting temperature within the operational range of the battery application (i.e. from 15 °C to 35 °C). However, a list of PCMs for BTM applications can be found in reference [38].

Research in PCM for BTMS applications generally focuses on: (i) using PCM as a passive system by investigating the effect of different parameters (e.g. type of PCM, PCM quantity amount) on the battery performance [39–52]; (ii) improving the poor thermal conductivity of PCMs by incorporating metal foams (e.g. Aluminium, copper and nickel foams) with PCMs [38,53,54], combining PCMs with metal fins [43,55,56], using composite PCMs [41,57,58], testing metal mesh and carbon-based materials such as expanded graphite (EG), carbon nanotubes (CNT), carbon fibre, with conventional PCM [39,59,60]; (iii) combining PCM with other transfer medium (e.g. air cooling [61,62], liquid cooling [63,64], or heat pipe cooling [65,66]). The findings indicate that these configurations may efficiently minimise the maximum temperature of the battery, assuring high efficiency, conserving cell temperature uniformity, and preventing thermal runaway [67]. Studies that have been proposed where PCM is combined with liquid cooling for batteries often use time-consuming CFD computational tools and do not analyse the system's functioning in continuous charging-discharging cycles (actual real-life battery operation) [68]. As a result, it is appropriate to use a fast-lumped model that can reliably forecast the behaviour of this linked PCM-liquid coolant [69].

To overcome these problems, Lamrani *et al.* [47] developed a simplified model to investigate a Li-ion battery pack with PCM-based BTMS and the maximum relative error of the numerical results obtained is approximately 6 % compared to experimental data from literature. Likewise, Lebrouhi *et al.* [70], developed a low-cost lumped model for simulating a Li-ion battery pack with thermal management systems (TMS) under continuous charging/discharging process and both the experimental results and the CFD findings were found to be in excellent agreement. Nevertheless, in these two models [47,70], the diffusion phenomenon, as well as the entropic term that reflects the reversible heat generated, were not included. The last aspect is frequently ignored in most literary works [71]. In addition, it is important to remember that the temperature homogeneity has a considerable impact on the performance of the battery pack. A temperature gradient between cells can lead to variations in the rate of electrochemical reactions, which can have a negative effect on the overall discharge/charge performance of the battery. Thermal stresses emanating from an irregular temperature distribution within a battery cell can also cause irreparable damage to the cell's performance and cycle stability. This can lead to reduced capacity, higher impedance, and self-discharge.

Therefore, it is essential to develop physical models capable of predicting temperature variations inside the battery equipped with a PCM throughout charge and discharge cycles. In this perspective, we have developed an improved version of the previously published model [70], aiming to integrate irreversible phenomena and thermal diffusion within batteries utilizing PCM as a thermal management system.

The objective of this article is to introduce this enhanced physical model to the scientific community interested in dynamic modelling of battery thermal management using phase-change materials. Notably, for this study, the New European driving cycle (NEDC) has been selected to assess the battery's response under real-world conditions within an electric vehicle, comprising four urban routes and one ultra-urban route. The proposed model has been validated using experimental data from literature. The investigation evaluates the influence of different parameters associated with characteristics of the utilised PCM and ambient conditions on the thermal behaviour of the battery pack.

2. Model development and validation

2.1. System description

The study addresses a specific battery pack including twenty-four 21700-cell Li-ion $LiNiMnCoAlO_2$ (NMC) cathode batteries arranged in a 6S4P configuration. The batteries are configured in series (6 cells per series) to attain the required voltage and in parallel (4 sets of 6 cells) to reach the desired output current. The choice of 21700-cell Li-ion NMC cathode batteries is based on their recent commercial appeal and elevated energy density. With over 50 % more energy per cell, these batteries have a substantially higher capacity than the typical 18,650 cylindrical cells. To regulate temperature disparity and enhance heat dissipation of the battery pack during charging/discharging cycles, PCM is integrated around the cells. Its function is to control the heat generated by the batteries.

The PCM integration prevents overheating, which is important since the battery performance, lifespan, and safety are affected by excessive heat. The present study emphasises the role of PCM-based BTMS in ensuring the optimal functioning of the battery pack and guaranteeing its safe and efficient operation. Fig. 2, illustrates the arrangement and configuration of the battery pack addressed in this study, highlighting the series and parallel connections of the 24 NMC cathode batteries. Each battery cell has a mass of 69 g and a nominal capacity of 4 Ah, as indicated in Table 1. The battery pack is 21.7 cm by 14.46 cm and 7.09 in height. It is important to note that in this study four distinct PCMs are investigated with disparate properties as given in Table 2.

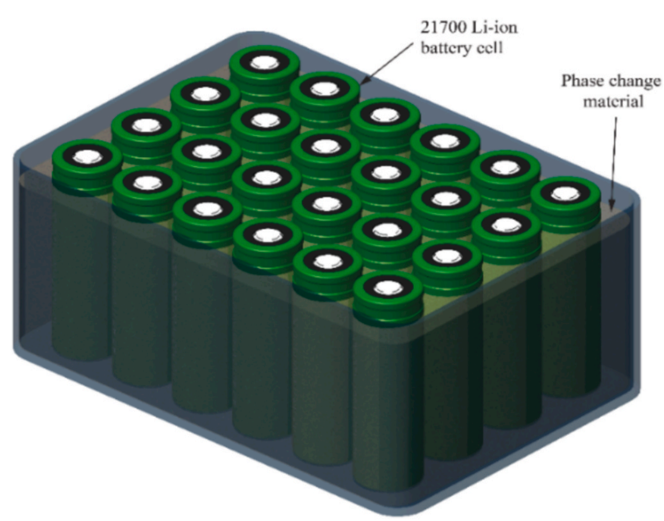

Fig. 2. The considered Li-Ion battery pack with its thermal management system.

Table 1
Characteristics of battery cells.

Property	Value
Mass (g)	69 ± 2
Diameter (mm)	21.7 ± 0.2
Height (mm)	70.9 ± 0.2
Nominal capacity (Ah)	4 Ah
Nominal voltage (V)	3.65 V

Table 2
Characteristics of PCM.

Property	RT28 HC	RT31	RT35 HC	RT42
Density of PCM (kg/m^3)	770/880	760/880	770/880	760/880
Heat capacity of PCM (kJ/kgK)	2	2	2	2
Thermal conductivity of PCM (W/mK)	0.2	0.2	0.2	0.2
Heat of fusion of PCM (kJ/kg)	250	165	240	165
Melting range of PCM (°C)	27–29	27–33	34–36	38–43

2.2. Modelling methodology

The current research introduces a new battery pack and thermal management system modelling methodology. This strategy relies on a fast-detailed lumped model to balance computing performance and accuracy. This approach fragments the battery pack into control volumes (CVij) (see Fig. 3). Each control volume represents a specific region within the battery pack and contains one battery cell enclosed by a PCM. During PCM phase transition the thermal energy is either accumulated or released from the operated battery pack. Dividing the battery module into control volumes allows the model to capture the internal spacio-temporal temperature variations. This enables an advanced representation of the pack in contrast to conventional lumped models, which presume a uniform temperature distribution throughout the entire pack. The new fast-detailed lumped model takes advantage of lumped modelling, simplifying the intricate geometry into interconnected control volumes. Prior study shows that cylindrical Li-ion cells have different thermal conductivity in axial and radial directions, with 99.1 % of heat dissipation occurring radially. This heat flux directionality demonstrates that a 2D radial would maintain high accuracy for BTMS with PCM [72].This reduces the computational complexity, and shortens the time needed for modelling and analysing. The developed model facilitates efficient and precise prediction of the thermal behaviour of the battery pack components, including individual cells and the PCM.

The detailed information on temperature distribution is crucial for customizing the BTMS, ensuring safe and efficient operation of the cell's module, while preventing thermal degradation and thermal runaway events.

By using the developed lumped approach, heat transfer in a battery pack can be represented using an electrical circuit analogy. This analogy allows us to understand and analyse the flow of heat within the pack using concepts similar to electrical circuits. In this analogy, the battery pack is represented as a network of resistors, capacitors, and heat sources (See Fig. 4). Each control volume (CVij) comprises two primary components: the battery cell and the PCM. The battery cell store and deliver electrical energy, during its operation the heat is generated as biproduct. Whereas the PCM absorbs and releases the excess cell heat generated to fulfil its role as thermal energy storage and transfer medium. Additionally, each control volume is associated with four heat ports (HPi). The HP associated represent the interfaces where thermal energy can be exchange between the control volume and its surroundings. The HPi can be categorized into two types:

- Heat input ports: These ports are utilized to deliver heat to the control volume. Heat can be transferred to the control volume from external sources, including the surrounding environment or other components within the battery pack. The heat input is essential for elevating the temperature of the control volume and its constituents.
- Heat output ports: These ports enable the removal of heat from the control volume. Heat may be transported from the control volume to the surrounding environment or to other cooling components. The heat emitted through these ports aids in lowering the temperature within the control volume.

Throughout the HP interface the model simulates the heat transfer between the cells, PCM, and their surroundings, allowing for a comprehensive analysis of the thermal behaviour and performance of the battery pack and its BTMS. To predict the temperature variation at each control volume, the transient energy balance for both the battery and the PCM domain is used through considering two capacitors (See Fig. 5). These transient energy balances for each control volume can be expressed as the following:

- ***Control volume 11 (CV_{11})***

–For the battery cell:

$$(mC_p)_{b11}\frac{\partial T_{b11}}{\partial t} = P_{gene,11} + \frac{(T_{pcm11} - T_{b11})}{R_{b-p}} \tag{1}$$

Where R_{b-p} is the conductive thermal resistance between the battery cell and the PCM. $P_{gene,11}$ is the heat generated by the cell battery in the control volume *11* given as the following:

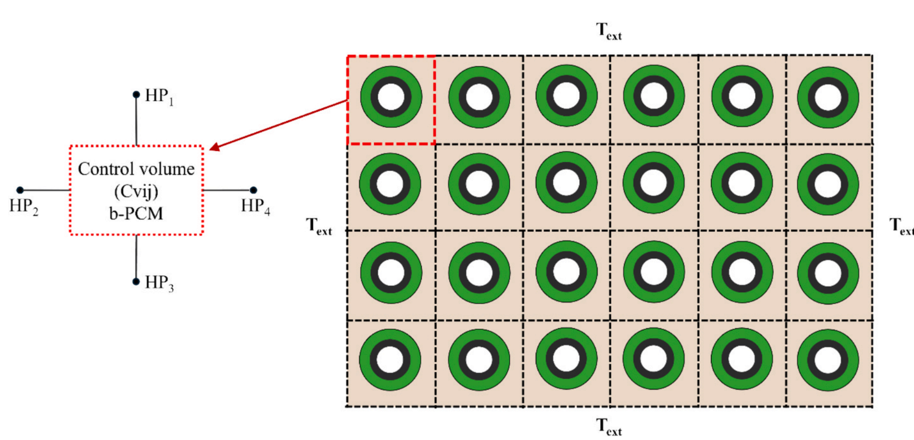

Fig. 3. Lumped modelling strategy of the battery pack with PCM.

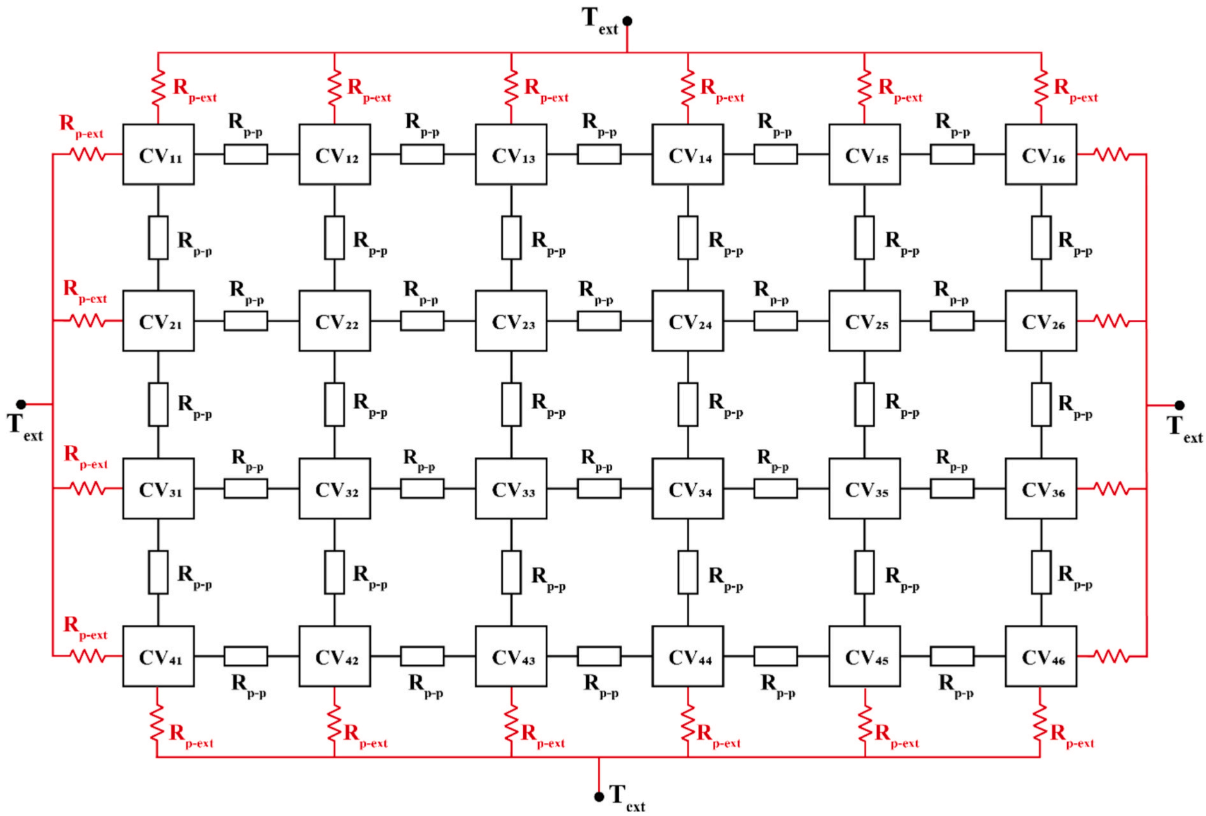

Fig. 4. Analogical schema of the heat transfer in the battery pack.

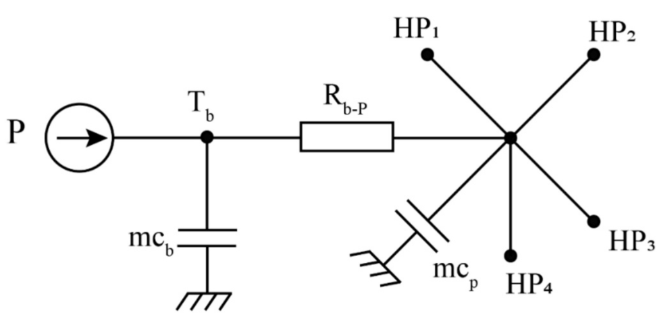

Fig. 5. Analogical heat transfer scheme for one control volume.

$$P_{gene,11} = R_{11}I^2 - IT_{b11}\Delta S\frac{1}{nF} \tag{2}$$

I. Is the used current and R_{11} is the internal resistance of the cell expressed as a function of the cell temperature [73]

$$R_{11}[\Omega] = \left[12.407 - 0.5345T_{b11} + 0.0134{T_{b11}}^2 - 0.0001{T_{b11}}^3\right] \times 10^{-3} \tag{3}$$

It is interesting to note that the used entropy variation (ΔS) is determined during the resolution of all coupled equations and it depends on the battery cell SoC[74]:

$$\Delta S = \begin{cases} 99.88SOC - 76.67 for 0 \leq SOC \leq 0.77 \\ 30 for 0.77 < SOC \leq 0.87 \\ -20 for 0.87 < SOC \leq 1 \end{cases} \tag{4}$$

For PCM:

$$(mC_p)_{pcm11}\frac{\partial T_{pcm11}}{\partial t} = \frac{(T_{b11} - T_{pcm11})}{R_{b-p}} + \frac{(T_{pcm12} - T_{pcm11})}{R_{cd(pcm11-pcm12)}} + \frac{(T_{pcm21} - T_{pcm11})}{R_{cd(pcm11-pcm21)}} + \frac{2(T_{ext} - T_{pcm11})}{R_{cv(pcm11-ext)}} \tag{5}$$

Where $R_{cd(pcm11-pcm12)}$ is the conductive thermal resistance between the PCM located in the control volume (CV_{11}) and the control volume (CV_{12}). $R_{cv(pcm11-ext)}$ is the convective thermal resistance between the PCM in the control volume (11) and the exterior ambient Refer to Fig. 4 for more details. The PCM's equivalent heat capacity is obtained following the methodology described in previous studies [47,70].

The methodology described earlier is applied to all 24 control volumes in the system. The control volumes can be categorized into two types based on their heat exchange characteristics. The first type is similar to CV_{11}, where heat exchange occurs between the control volume and both the exterior ambient and the surrounding PCM. In these control volumes, the methodology involves calculating both the conductive thermal resistance (R_{cd}) between the PCM within the control volume and the surrounding PCM, as well as the convective thermal resistance (R_{cv}) between the PCM and the exterior ambient. The second type of control volume is in contact only with PCMs from the surrounding control volumes; this type does not directly exchange heat with the exterior ambient. Furthermore, the procedure focuses on calculating the conductive thermal resistance (R_{cd}) between the PCM within the control volume and the PCM in adjacent control volume. Overall, the approach considers the heat transfer characteristic of each control volume and, depending on the form of heat exchange involved, determines the proper thermal resistances. Differentiating between the two kinds of control volumes facilitates the calculation of the system's applicable thermal resistance.

As an example of the applied energy balance on the second type of control volume, CV_{24} is considered and the used transient equations to determine the temperature variation can be given as the following:

–***For the battery cell (CV_{24}):***

$$(mC_p)_{b24}\frac{\partial T_{b24}}{\partial t} = P_{gene,24} + \frac{(T_{pcm24} - T_{b24})}{R_{b-p}} \tag{6}$$

– ***For PCM (CV_{24}):***

$$(mC_p)_{pcm24}\frac{\partial T_{pcm24}}{\partial t} = \frac{(T_{b24} - T_{pcm24})}{R_{b-p}} + \frac{(T_{pcm14} - T_{pcm24})}{R_{cd(pcm24-pcm14)}} + \frac{(T_{pcm34} - T_{pcm24})}{R_{cd(pcm24-pcm34)}} + \frac{(T_{pcm23} - T_{pcm24})}{R_{cd(pcm24-pcm23)}} + \frac{(T_{pcm25} - T_{pcm24})}{R_{cd(pcm24-pcm25)}} \tag{7}$$

2.3. Model validation

The generated model's accuracy was determined by comparing the obtained numerical findings with published experimental and CFD data [63]. Multiple charging and discharging cycles were performed on the battery cell using PCM as the TMS in the experiments. The used cell is rated at 4 Ah nominally. PCM was used to insulate this battery pack, which was set at 30 °C to begin with. The pack of batteries was given a 0.5-C charge and a 3-C discharge. C-rate, which measures the charge and release current relative to nominal capacity, is an intriguing metric to consider. The suggested lumped model used the prior experimental settings as input parameters, and the predicted temperature of the battery and the observed one are shown in Fig. 6. It can be shown that the CFD findings from Ref [63] and the experimental data are in excellent agreement with the suggested model. The proposed lumped model yields to an error of 2 °C between observed and simulated battery temperature, with an average absolute error of 0.27 °C and a root means square error of 0.39 °C. These findings clearly demonstrate that, in comparison to the time-consuming CFD tools, the use of a rapid and reduced coupled model for pack TMS is appropriate and able to forecast with reasonable precision the actual performance of the battery TMS.

3. Results and discussion

To investigate the dynamic thermal behaviour of the battery under real-world conditions, the integration of the NEDC into the physical simulations was executed. The NEDC comprises four urban cycles and one ultra-urban cycle, as visually represented in Fig. 7. The combined duration of these four cycles amounts to approximately 1200 s. To replicate authentic usage patterns, the NEDC is executed three times, each separated by 600 s, allowing for intervals of rest between complete charging and discharging cycles. As shown in Fig. 8, the updated version of the thermal model provides precise predictions of the battery pack's SoC throughout its operation. Initially, before the rapid discharge process begins, the battery pack is assumed to be at full charge. As mentioned in the reference [75], the vehicle's velocity is directly proportional to the battery rate of discharge. Once the battery pack is fully discharged, a constant current of 12 A is applied during the charging process, raising the SoC to 100 %. An additional resting period of 600 s is introduced between each charging/discharging cycle, where the SoC is stabilize at 100 % as depicted in Fig. 8. The battery pack undergoes the aforementioned charging and discharging process utilising a passive PCM-BTMS.

The heat generation profile within the battery pack is illustrated in Fig. 9, demonstrating the evolution of heat during this process. Upon examining this figure, it becomes evident that the battery temperature gradually rises during each urban cycle, followed by a rapid increase during each ultra-urban cycle, reaching its peak value. Subsequently, the temperature decreases during the charging process and remains stable throughout this phase.

To investigate the impact of design and operational factors on the battery pack and its thermal management system, a comprehensive

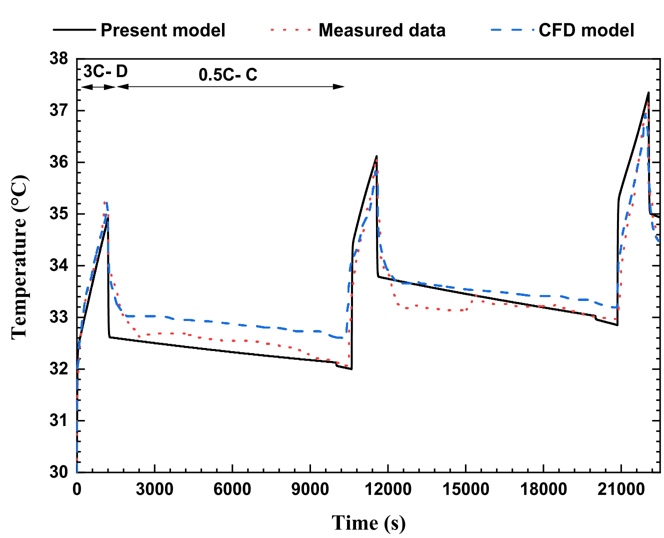

Fig. 6. Comparison of the current model, experimental data, and CFD findings obtained from Ref [63].

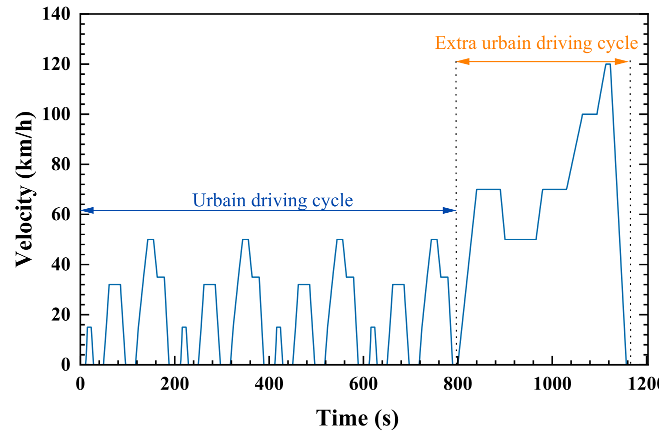

Fig. 7. New European Driving Cycle.

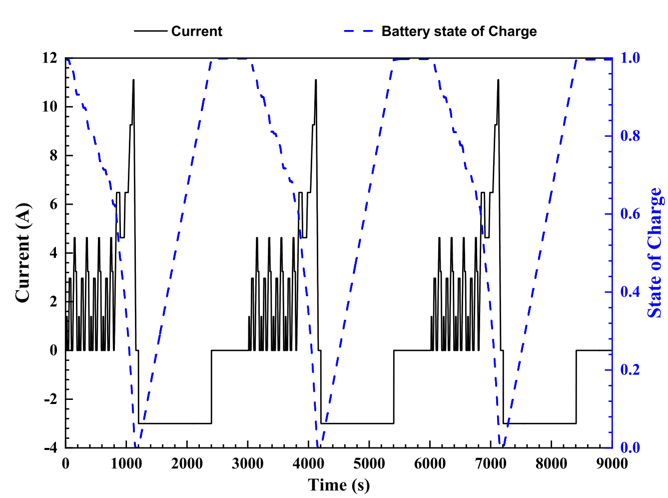

Fig. 8. Applied current (NEDC) per cell and SOC of batteries.

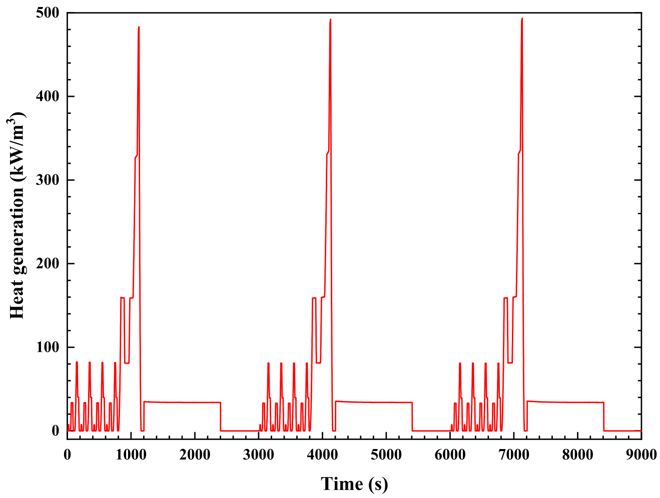

Fig. 9. Heat generation profile per cell in the battery pack.

parametric study was carried out. The study employed the proposed thermal model, and the subsequent findings are presented and analysed in the forthcoming sections.

3.1. PCM effect

To assess the impact of different PCMs on battery thermal management performance, an investigation was conducted on four distinct commercial PCMs (RT-28HC, RT 31, RT35 HC, RT 42) as detailed in reference [76]. The temperature fluctuations of the battery pack during both charging and discharging cycles are presented in Fig. 10-**a** as the outcomes of this study. To quantify the maximum thermal gradients within the battery during the solid–liquid phase change process, temperature variations were analysed at two locations: at the center of the pack and at a point near the pack's outer air interface (specifically, at the pack's corner). The intermediate control volume temperature falls between these two bounds. The use of PCM RT-28HC and RT-28HC as thermal management materials resulted in the battery achieving its lowest temperatures at both the corner and the center of the pack.

PCM RT-28HC and RT 31 intrinsic characteristics, particularly their latent heat, allow them to efficiently absorb a significant quantity of heat generated by the cells. As a result, the battery pack internal temperature remains low compared the other cases. It's important to note that RT35 HC and RT 42 do not undergo a phase transition in the first 3500 s,

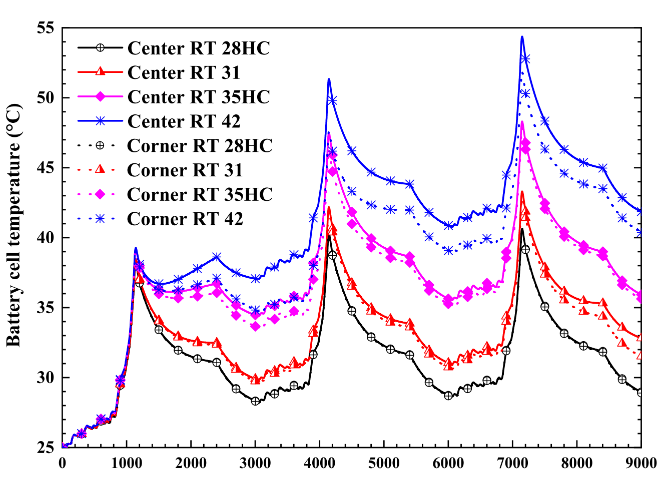

Fig. 10. Temporal variation of battery temperature at different location within the pack the center and corners of the pack.

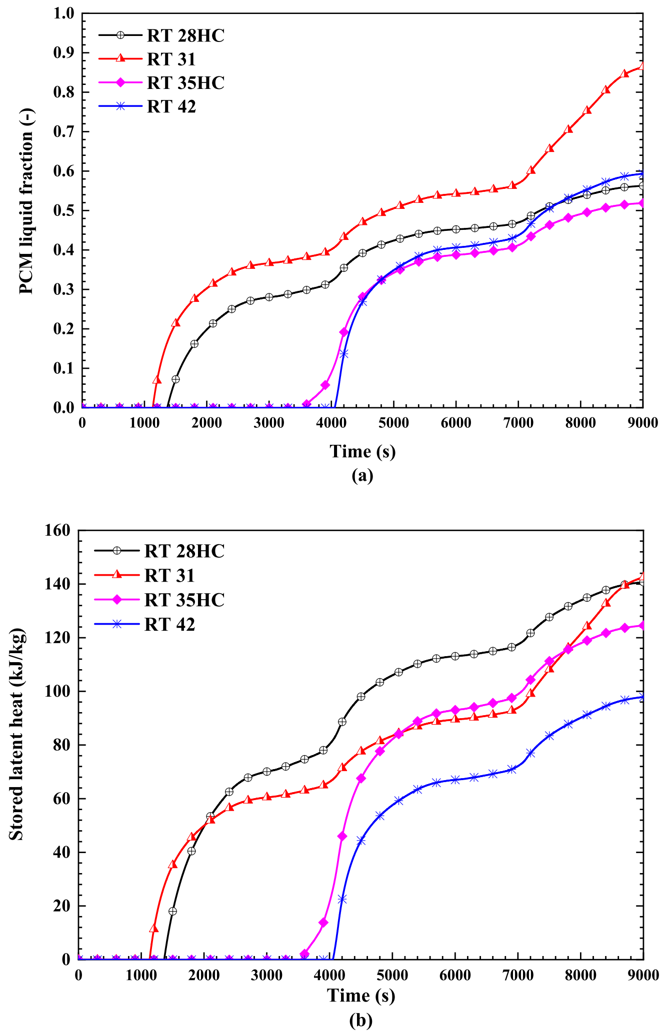

Fig. 11. **(a)** PCM liquid fraction and **(b)** Stored latent heat during the functioning of battery pack.

which leads to a reduced amount of heat accumulation through the sensible heat of the PCM. As a result, the module temperature rises impacting the performance in this period.

This behavior is corroborated by the data presented in Fig. 11-**a** and Fig. 11-**b**, which depict the liquid fraction of PCM and the accumulated latent heat during the battery pack's operation. It is evident that PCM RT-28HC and RT 31 initiate the phase change process rapidly, owing to their lower phase transition temperature, in contrast to RT35 HC and RT 42.

In addition to the variation in the maximum temperature within the battery pack, another crucial parameter that affects its operation is the variation in thermal gradient within the battery pack, as depicted in Fig. 12. This thermal gradient serves as an indicator to evaluate the level of temperature uniformity within the battery pack.

The results reveal that the utilisation of PCM RT-28HC maintains a nearly consistent temperature distribution within the battery. Conversely, for RT 31, the maximum temperature difference within the battery remains below 0.5 °C during the first three complete cycles but gradually increases afterward. In contrast, for RT35 HC, the maximum thermal gradient rapidly increases during the initial 4000 s, reaching almost 1.5 °C, before decreasing to values below 0.5 °C. However, it's essential to note that temperatures persist relatively high both at the center and in the corners, at approximately 48 °C.

It is important to note that it is not favoured to use a PCM with a transition temperature higher than 35 °C in the battery pack. This

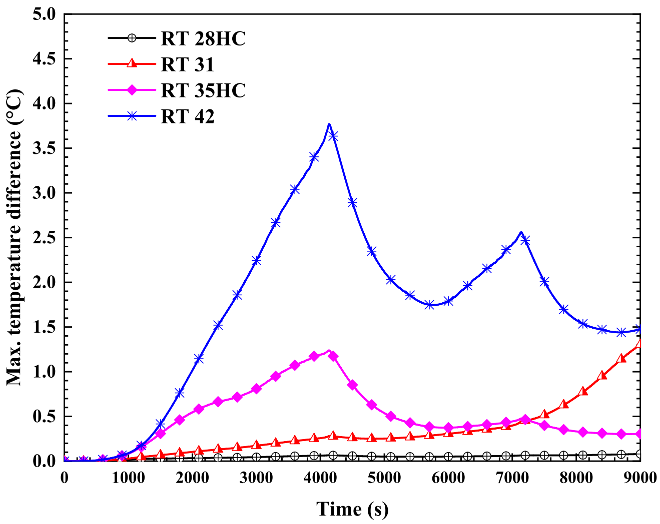

Fig. 12. Variation of maximal temperature difference in the battery pack.

recommendation is grounded from the outcomes disclosed during the charge and discharge cycles, which showed that the PCM is fully melted after the third cycle. As a result, it was less able to absorb heat from the batteries, hence the overall performance of thermal management was diminished.

In contrast, a BTMS based on PCM RT-28HC demonstrated prominent heat management functioning. While it provides effective cooling, it may not guarantee perfect temperature uniformity within the battery throughout the entire charge/discharge cycles.

To further support these findings, reference is made to Fig. 13, which provides insights on the heat generation within the battery pack for each kind of PCM, helps to further support the earlier findings. In comparison to RT35 HC and RT42, PCM RT-28HC and RT 31 both show a lower amounts of heat generation, as can be seen by closely examining Fig. 13. This corroborates our earlier conclusions regarding the effectiveness of these PCMs in managing heat generation. In conclusion, for effective thermal management of a battery pack, the transition temperature of the PCM should be considered a critical parameter.

In our case, PCM RT-28HC and RT 31 proved to be effective choices, while PCMs with higher transition temperatures like RT35 HC and RT 42 did not perform as effectively in absorbing and dissipating heat from the batteries during operation. This knowledge can guide the design and selection of thermal management systems for batteries in real-world applications, enhancing their overall performance and longevity.

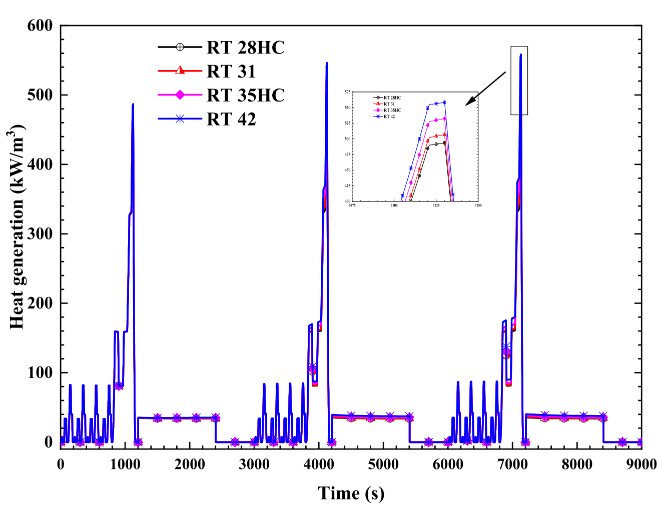

Fig. 13. Heat generation per cell: effect of PCM type.

3.2. Effect of air temperature

In this section, we investigate the impact of heat exchange between the battery pack equipped with PCM RT 28HC and its surrounding environment. The performance of the battery pack is examined throughout the charge/discharge cycle at different ambient temperatures, including 20 °C, 25 °C, 30 °C, 35 °C, and 40 °C, with the initial temperature of the pack set to 25 °C. The selected temperature values reflect the seasonal fluctuations conditions encountered in Europe, allowing for relevant and representative data for our analysis.

Fig. 14 illustrates the evolution of battery cell temperatures under diverse operational conditions, whereas Fig. 15 depicts the maximum temperature variation observed within the battery pack. Fig. 16**-a and 16-b** illustrate the liquid fraction of the PCM RT 28HC during the operation of the battery pack.

It is evident that the proposed BTMS effectively keeps the battery cells within the appropriate temperature range, despite external temperatures varying from 20 °C to 35 °C. The BTMS, incorporating RT 28HC, ensures that the battery cells maintain suitable temperatures while keeping an acceptable temperature gradient within the battery pack when the ambient temperature is below 35 °C. However, at external temperature of 40 °C, a notable increase in the temperature gradient within the battery pack is observed since the beginning of the cycle. Which later experiences a significant increase during the third cycle, especially after 7000 s.

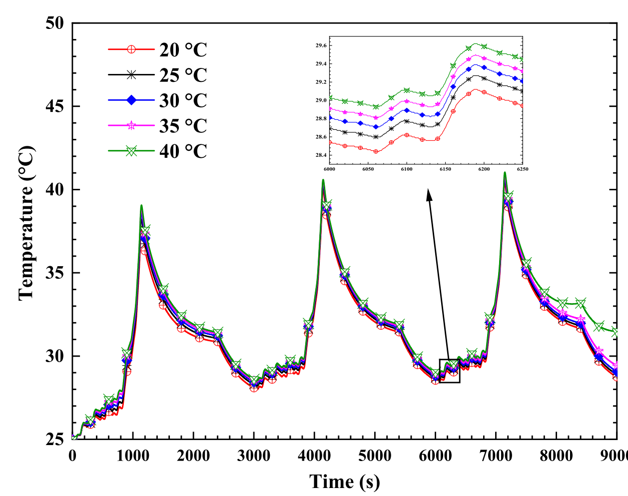

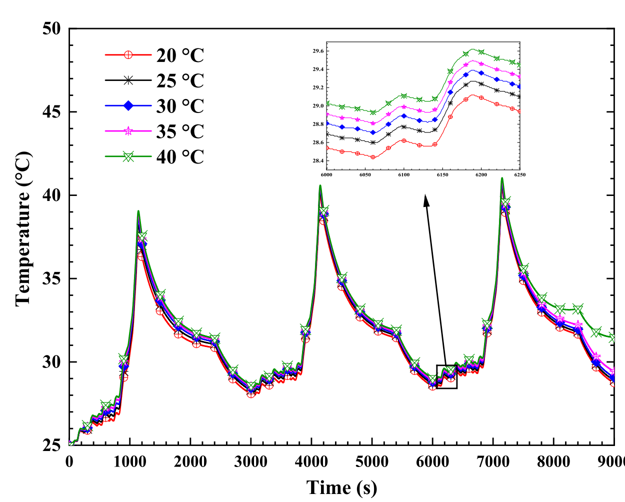

Fig. 14. Battery cell temperature at the corner of the pack.

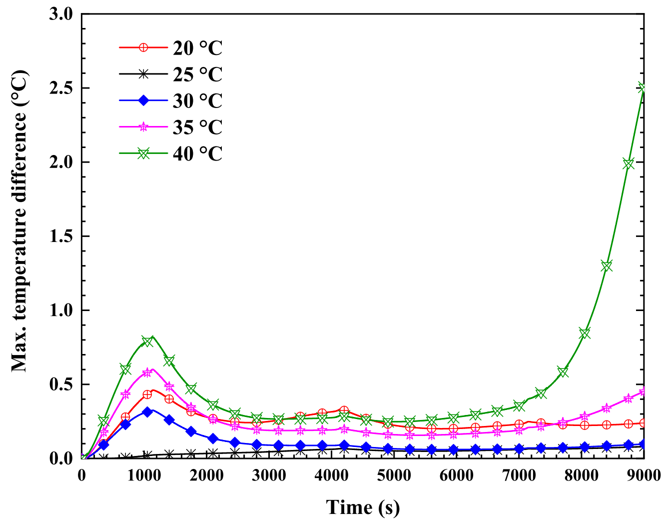

Fig. 15. Maximal temperature difference in the battery pack.

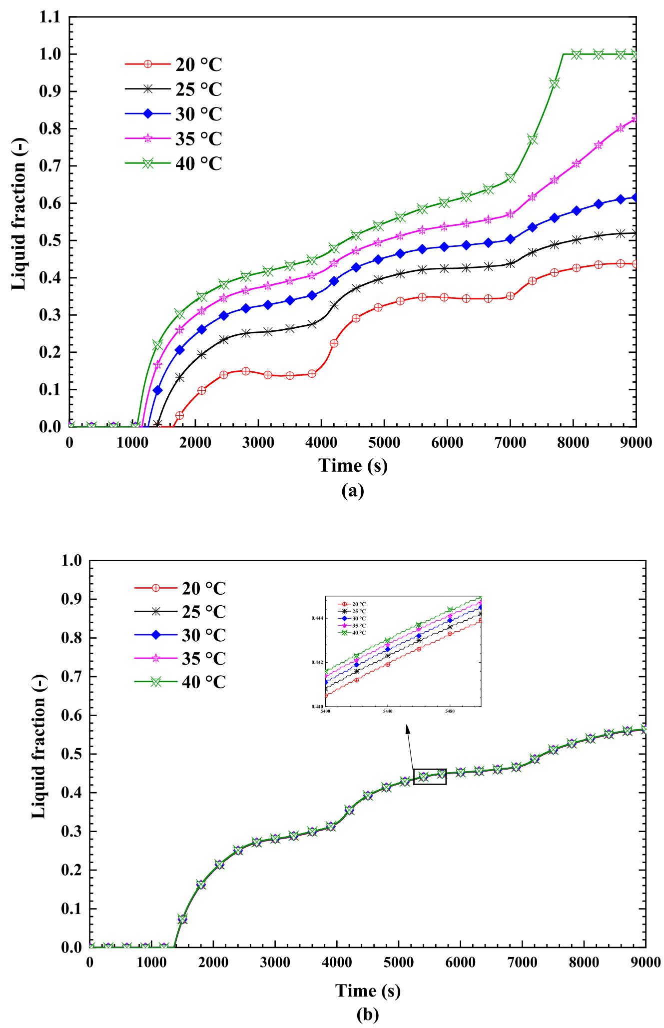

Fig. 16. Liquid fraction: (a) at the corner of the battery pack, (b) at the center of the pack.

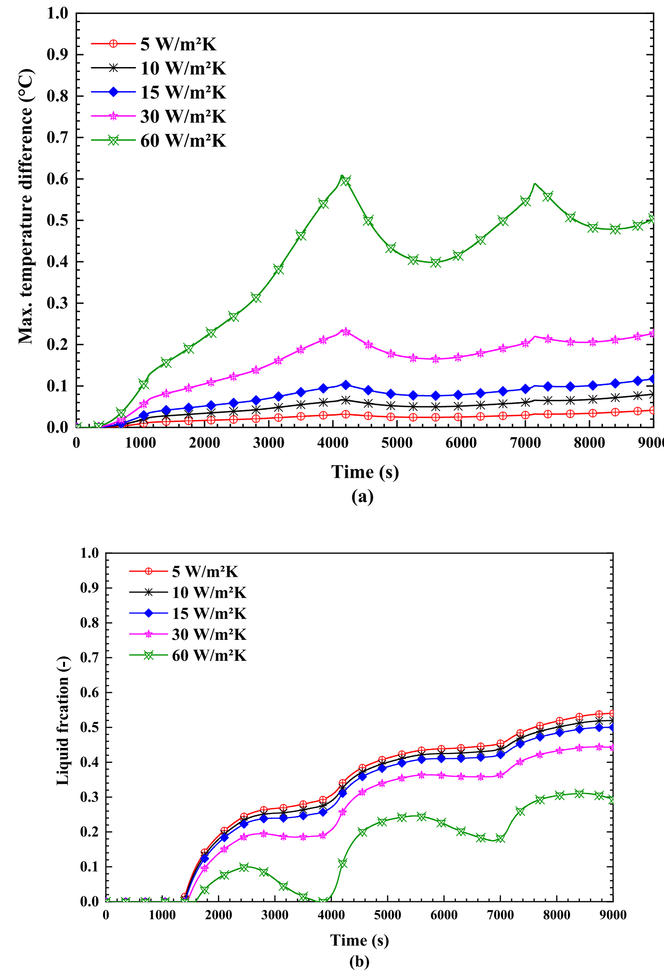

Fig. 17. (a) Maximum temperature difference and (b) Average PCM liquid fraction.

3.3. *Effect of ambient convective coefficient*

Fig. 17 illustrates the influence of the convective heat transfer coefficient between the battery pack and its external environment during the charge/discharge cycle on both the solid–liquid phase transition process of RT 28HC and the maximum thermal gradient within the pack. The convective heat transfer coefficient varies across a range from 5 W/m^2 K to 60 W/m^2 K.

Observations reveal that when the convective heat transfer coefficient falls within the range of 5 W/m^2 K to 30 W/m^2 K, the maximum thermal gradient within the battery pack remains below 0.25 °C. However, when the heat transfer coefficient equals or exceeds 60 W/m^2 K, significant thermal gradients within the pack become evident.

To address and mitigate these thermal gradients, it becomes essential to combine this passive PCM-based method with other thermal management systems, such as liquid cooling or air-cooling. These supplementary methods have the potential to further reduce the thermal gradient within the batteries, as indicated by reference [70].

4. Conclusion

In this paper an improved version of a basic physical model that we previously presented to analyse the energy efficiency of a thermal management system based on a phase change material (PCM) for Li-ion batteries. The updated model incorporates irreversible phenomena as well as two-dimensional thermal diffusion. For this study, we opted for the NEDC, which represents the actual use of an electric vehicle on four urban routes and one ultra-urban route. The validity of the proposed model was confirmed through validation against experimental data available in the literature. Our detailed analysis explored the influence of several parameters on the thermal behaviour of the battery pack. The proposed model accurately describes heat transfer and temperature distribution within the battery during the liquid-to-solid phase change process, as the finding reveals. It's important to note that under specific operating conditions, the thermal gradient within the battery pack remains within acceptable safety limits. However, in certain scenarios, the adoption of a thermal management system that combines PCM with active cooling is necessary to reduce thermal gradients and maintain temperature uniformity within the battery pack.

In conclusion, this new model provides an efficient and cost-effective alternative to computationally intensive CFD methods for analysing the thermal dynamic behaviour of batteries with embedded PCMs over prolonged charge and discharge cycles. Moreover, future research will be centred on the extension of the existing model to the three dimensions, using a lumped element approach and integrating localized heat generation model. Such a model can then be used to compare the different BTMS configurations used in industry.

CRediT authorship contribution statement

A. Afass: Writing – original draft, Software, Methodology, Investigation. **B. Lamrani:** Validation, Software, Investigation, Formal analysis. **B. Lebrouhi:** Writing – original draft, Validation, Software, Methodology. **M.A. Tankari:** Writing – review & editing, Supervision, Methodology. **M. Karkri:** Writing – review & editing, Supervision, Methodology. **S. Landini:** Writing – review & editing, Supervision, Methodology. **T. Kousksou:** Writing – review & editing, Supervision, Project administration.

Declaration of competing interest

The authors declare that they have no known competing financial interests or personal relationships that could have appeared to influence the work reported in this paper.

Acknowledgments

This project has received funding from the European Union's Horizon 2020 research and innovation programme under the Marie Skłodowska-Curie grant agreement No 945416.

Data availability

Data will be made available on request.

References

[1] Net Zero by 2050 – Analysis - IEA n.d. https://www.iea.org/reports/net-zero-by-2050 (accessed November 8, 2022).
[2] Lebrouhi BE, Schall E, Lamrani B, Chaibi Y, Kousksou T. Energy Transition in France. Sustainability (switzerland) 2022;14. https://doi.org/10.3390/su14105818.
[3] Lebrouhi BE, Khattari Y, Lamrani B, Maaroufi M, Zeraouli Y, Kousksou T. Key challenges for a large-scale development of battery electric vehicles : A comprehensive review. J Energy Storage 2021;44:103273. https://doi.org/10.1016/j.est.2021.103273.
[4] Liu Y, Dong F. What are the roles of consumers, automobile production enterprises, and the government in the process of banning gasoline vehicles? Evidence from a tripartite evolutionary game model. Energy 2022;238:122004. https://doi.org/10.1016/J.ENERGY.2021.122004.
[5] Benvenutti LMM, Ribeiro AB, Uriona M. Long term diffusion dynamics of alternative fuel vehicles in Brazil. J Clean Prod 2017;164:1571–85. https://doi.org/10.1016/J.JCLEPRO.2017.07.051.
[6] Logan KG, Nelson JD, Lu X, Hastings A. UK and China: Will electric vehicle integration meet Paris Agreement Targets? Transp Res Interdiscip Perspect 2020;8:100245. https://doi.org/10.1016/J.TRIP.2020.100245.
[7] Yue QL, He CX, Wu MC, Zhao TS. Advances in thermal management systems for next-generation power batteries. Int J Heat Mass Transf 2021;181:121853. https://doi.org/10.1016/J.IJHEATMASSTRANSFER.2021.121853.
[8] Shahid S, Agelin-Chaab M. A review of thermal runaway prevention and mitigation strategies for lithium-ion batteries. Energy Convers Manage: X 2022;16:100310. https://doi.org/10.1016/j.ecmx.2022.100310.
[9] Sun P, Bisschop R, Niu H, Huang X. A Review of Battery Fires in Electric Vehicles. Fire Technol 2020;56:1361–410. https://doi.org/10.1007/S10694-019-00944-3/FIGURES/26.
[10] Tesla. First Responders Information. TESLA MODEL S ELECTRIC 2016. https://www.tesla.com/firstresponders#firstresponders (accessed November 8, 2022).
[11] Lin X, Khosravinia K, Hu X, Li J, Lu W. Lithium Plating Mechanism, Detection, and Mitigation in Lithium-Ion Batteries. Prog Energy Combust Sci 2021;87:100953. https://doi.org/10.1016/J.PECS.2021.100953.
[12] Landini S, O'Donovan TS. Experimental investigation of lithium-ion cells ageing under isothermal conditions for optimal lifetime performance. J Energy Storage 2022;48:103680. https://doi.org/10.1016/j.est.2021.103680.
[13] Landini S, Leworthy J, O'Donovan TS. A Review of Phase Change Materials for the Thermal Management and Isothermalisation of Lithium-Ion Cells. J Energy Storage 2019;25:100887. https://doi.org/10.1016/j.est.2019.100887.
[14] Landini S, O'Donovan TS. Novel experimental approach for the characterisation of Lithium-Ion cells performance in isothermal conditions. Energy 2021;214:118965. https://doi.org/10.1016/j.energy.2020.118965.
[15] Hamed MM, El-Tayeb A, Moukhtar I, El Dein AZ, Abdelhameed EH. A review on recent key technologies of lithium-ion battery thermal management: External cooling systems. Results Eng 2022;16:100703. https://doi.org/10.1016/j.rineng.2022.100703.
[16] Ma S, Jiang M, Tao P, Song C, Wu J, Wang J, et al. Temperature effect and thermal impact in lithium-ion batteries: A review. Prog Nat Sci: Mater Int 2018;28:653–66. https://doi.org/10.1016/J.PNSC.2018.11.002.
[17] Shu X, Yang W, Guo Y, Wei K, Qin B, Zhu G. A reliability study of electric vehicle battery from the perspective of power supply system. J Power Sources 2020;451:227805. https://doi.org/10.1016/j.jpowsour.2020.227805.
[18] Beauregard GP, Phoenix AZ. Report of investigation: Hybrids plus plug in hybrid electric vehicle. National Rural Electric Cooperative Association, Inc and US Department of Energy, Idaho National Laboratory by Etec, Online Im Internet: URL: Http://Www Evworld Com/Library/Prius_fire_forensics Pdf [Stand 1104 2012] 2008.
[19] Kim J, Oh J, Lee H. Review on battery thermal management system for electric vehicles. Appl Therm Eng 2019;149:192–212. https://doi.org/10.1016/j.applthermaleng.2018.12.020.
[20] Mehta R, Gupta A. Mathematical modelling of electrochemical, thermal and degradation processes in lithium-ion cells—A comprehensive review. Renew Sustain Energy Rev 2024;192:114264. https://doi.org/10.1016/j.rser.2023.114264.
[21] Zichen W, Changqing D. A comprehensive review on thermal management systems for power lithium-ion batteries. Renew Sustain Energy Rev 2021;139:110685. https://doi.org/10.1016/j.rser.2020.110685.
[22] Tran MK, Panchal S, Khang TD, Panchal K, Fraser R, Fowler M. Concept Review of a Cloud-Based Smart Battery Management System for Lithium-Ion Batteries: Feasibility, Logistics, and Functionality. Batteries 2022, Vol 8, Page 19 2022;8:19. doi: 10.3390/BATTERIES8020019.
[23] Akkaldevi C, Chitta SD, Jaidi J, Panchal S, Fowler M, Fraser R. Coupled Electrochemical-Thermal Simulations and Validation of Minichannel Cold-Plate Water-Cooled Prismatic 20 Ah LiFePO4 Battery. Electrochem 2021, Vol 2, Pages 643-663 2021;2:643–63. doi: 10.3390/ELECTROCHEM2040040.
[24] Li X, Zhao J, Duan J, Panchal S, Yuan J, Fraser R, et al. Simulation of cooling plate effect on a battery module with different channel arrangement. J Energy Storage 2022;49:104113. https://doi.org/10.1016/J.EST.2022.104113.
[25] Tran MK, Cunanan C, Panchal S, Fraser R, Fowler M. Investigation of Individual Cells Replacement Concept in Lithium-Ion Battery Packs with Analysis on Economic Feasibility and Pack Design Requirements. Processes 2021, Vol 9, Page 2263 2021;9:2263. doi: 10.3390/PR9122263.
[26] Mali V, Saxena R, Kumar K, Kalam A, Tripathi B. Review on battery thermal management systems for energy-efficient electric vehicles. Renew Sustain Energy Rev 2021;151:111611. https://doi.org/10.1016/J.RSER.2021.111611.
[27] Benabdelaziz K, Lebrouhi B, Maftah A, Maaroufi M. Novel external cooling solution for electric vehicle battery pack. Energy Rep 2019;6:262–72. https://doi.org/10.1016/j.egyr.2019.10.043.
[28] Tete PR, Gupta MM, Joshi SS. Developments in battery thermal management systems for electric vehicles: A technical review. J Energy Storage 2021;35:102255. https://doi.org/10.1016/j.est.2021.102255.
[29] Solai E, Capurso T, Khelladi S. Numerical study of a novel jet-grid approach for Li-ion batteries cooling. Energy Convers Manage: X 2025;25:100832. https://doi.org/10.1016/j.ecmx.2024.100832.
[30] Lin X-W, Li Y-B, Wu W-T, Zhou Z-F, Chen B. Advances on two-phase heat transfer for lithium-ion battery thermal management. Renew Sustain Energy Rev 2024;189:114052. https://doi.org/10.1016/j.rser.2023.114052.
[31] Lin X-W, Zhou Z-F, Yin J, Zhu X-G, Shi M-Y, Chen B. A comparative investigation of two-phase immersion thermal management system for lithium-ion battery pack. J Clean Prod 2024;434:140472. https://doi.org/10.1016/j.jclepro.2023.140472.

[32] Wu W, Wang S, Wu W, Chen K, Hong S, Lai Y. A critical review of battery thermal performance and liquid based battery thermal management. Energy Convers Manag 2019;182:262–81. https://doi.org/10.1016/j.enconman.2018.12.051.
[33] Lin J, Liu X, Li S, Zhang C, Yang S. A review on recent progress, challenges and perspective of battery thermal management system. Int J Heat Mass Transf 2021;167:120834. https://doi.org/10.1016/j.ijheatmasstransfer.2020.120834.
[34] Lin X-W, Zhou Z-F, Liu T-F, Xue S-Q, Liang Y, Zhang L-F, et al. Rate capability and Ragone plots for designing battery thermal management system based on phase change material. J Energy Storage 2023;74:109539. https://doi.org/10.1016/j.est.2023.109539.
[35] Ling Z, Cao J, Zhang W, Zhang Z, Fang X, Gao X. Compact liquid cooling strategy with phase change materials for Li-ion batteries optimized using response surface methodology. Appl Energy 2018;228:777–88. https://doi.org/10.1016/j.apenergy.2018.06.143.
[36] Subramanian M, Hoang AT, B K, Nižetić S, Soloman JM, Balasubramanian D,, et al. A technical review on composite phase change material based secondary assisted battery thermal management system for electric vehicles. J Clean Prod 2021:129079. https://doi.org/10.1016/J.JCLEPRO.2021.129079.
[37] Srivastava G, Nandan R, Das MK. Thermal runaway management of Li ion battery using PCM: A parametric study. Energy Convers Manage: X 2022;16:100306. https://doi.org/10.1016/j.ecmx.2022.100306.
[38] Babu Sanker S, Baby R. Phase change material based thermal management of lithium ion batteries: A review on thermal performance of various thermal conductivity enhancers. J Energy Storage 2022;50:104606. https://doi.org/10.1016/j.est.2022.104606.
[39] Babapoor A, Azizi M, Karimi G. Thermal management of a Li-ion battery using carbon fiber-PCM composites. Appl Therm Eng 2015;82:281–90. https://doi.org/10.1016/j.applthermaleng.2015.02.068.
[40] Wu W, Wu W, Wang S. Thermal optimization of composite PCM based large-format lithium-ion battery modules under extreme operating conditions. Energy Convers Manag 2017;153:22–33. https://doi.org/10.1016/j.enconman.2017.09.068.
[41] Wu W, Liu J, Liu M, Rao Z, Deng H, Wang Q, et al. An innovative battery thermal management with thermally induced flexible phase change material. Energy Convers Manag 2020;221:113145. https://doi.org/10.1016/j.enconman.2020.113145.
[42] El Idi MM, Karkri M, Abdou TM. A passive thermal management system of Li-ion batteries using PCM composites: Experimental and numerical investigations. Int J Heat Mass Transf 2021;169:120894. https://doi.org/10.1016/j.ijheatmasstransfer.2020.120894.
[43] Ping P, Peng R, Kong D, Chen G, Wen J. Investigation on thermal management performance of PCM-fin structure for Li-ion battery module in high-temperature environment. Energy Convers Manag 2018;176:131–46. https://doi.org/10.1016/j.enconman.2018.09.025.
[44] Sun Z, Fan R, Zheng N. Thermal management of a simulated battery with the compound use of phase change material and fins: Experimental and numerical investigations. Int J Therm Sci 2021;165:106945. https://doi.org/10.1016/j.ijthermalsci.2021.106945.
[45] Wang Y, Wang Z, Min H, Li H, Li Q. Performance investigation of a passive battery thermal management system applied with phase change material. J Energy Storage 2021;35:102279. https://doi.org/10.1016/j.est.2021.102279.
[46] Galazutdinova Y, Ushak S, Farid M, Al-Hallaj S, Grágeda M. Development of the inorganic composite phase change materials for passive thermal management of Li-ion batteries: Application. J Power Sources 2021;491:229624. https://doi.org/10.1016/j.jpowsour.2021.229624.
[47] Lamrani B, Lebrouhi BE, Khattari Y, Kousksou T. A simplified thermal model for a lithium-ion battery pack with phase change material thermal management system. J Energy Storage 2021;44:103377. https://doi.org/10.1016/J.EST.2021.103377.
[48] Jiang K, Liao G, E J, Zhang F, Chen J, Leng E.. Thermal management technology of power lithium-ion batteries based on the phase transition of materials: A review. J Energy Storage 2020;32:101816. https://doi.org/10.1016/j.est.2020.101816.
[49] Liu Z, Huadan C, Wang B, Li P. Coupling optimization of protruding fin and PCM in hybrid cooling system and cycle strategy matching for lithium-ion battery thermal management. Int J Therm Sci 2025;207:109372. https://doi.org/10.1016/j.ijthermalsci.2024.109372.
[50] Sutheesh PM, Jose J, Hotta TK, Rohinikumar B. Numerical investigations on thermal performance of PCM-based lithium-ion battery thermal management system equipped with advanced honeycomb structures. Int Commun Heat Mass Transfer 2024;158:107937. https://doi.org/10.1016/j.icheatmasstransfer.2024.107937.
[51] Landini S, Delgado-Diaz W, Ravotti R, Waser R, Stamatiou A, Worlitschek J, et al. Effect of geometry and thermal mass of Direct-Metal-Laser-Sintered aluminium Heat Exchangers filled with phase change materials on Lithium-Ion cells' passive cooling. Appl Therm Eng 2021;195:117151. https://doi.org/10.1016/j.applthermaleng.2021.117151.
[52] Landini S, Waser R, Stamatiou A, Ravotti R, Worlitschek J, O'Donovan TS. Passive cooling of Li-Ion cells with direct-metal-laser-sintered aluminium heat exchangers filled with phase change materials. Appl Therm Eng 2020;173:115238. https://doi.org/10.1016/j.applthermaleng.2020.115238.
[53] Situ W, Zhang G, Li X, Yang X, Wei C, Rao M, et al. A thermal management system for rectangular LiFePO4 battery module using novel double copper mesh-enhanced phase change material plates. Energy 2017;141:613–23. https://doi.org/10.1016/J.ENERGY.2017.09.083.
[54] Lin J, Liu D, Liu X, Liu M, Cui Y. CNT@MXene porous composite PCM based thermal management for lithium-ion battery system. Appl Therm Eng 2025;262:125240. https://doi.org/10.1016/j.applthermaleng.2024.125240.
[55] Shojaeefard MH, Molaeimanesh GR, Ranjbaran YS. Improving the performance of a passive battery thermal management system based on PCM using lateral fins. Heat and Mass Transfer 2019 55:6 2019;55:1753–67. doi: 10.1007/S00231-018-02555-0.
[56] Ismail M, Panter JR, Landini S. Numerical investigation of fin geometries on the effectiveness of passive, phase-change material −based thermal management systems for lithium-ion batteries. Appl Therm Eng 2025;262:125216. https://doi.org/10.1016/j.applthermaleng.2024.125216.
[57] Wang W, Zhang X, Xin C, Rao Z. An experimental study on thermal management of lithium ion battery packs using an improved passive method. Appl Therm Eng 2018;134:163–70. https://doi.org/10.1016/J.APPLTHERMALENG.2018.02.011.
[58] Jiang G, Huang J, Liu M, Cao M. Experiment and simulation of thermal management for a tube-shell Li-ion battery pack with composite phase change material. Appl Therm Eng 2017;120:1–9. https://doi.org/10.1016/J.APPLTHERMALENG.2017.03.107.
[59] Samimi F, Babapoor A, Azizi M, Karimi G. Thermal management analysis of a Li-ion battery cell using phase change material loaded with carbon fibers. Energy 2016;96:355–71. https://doi.org/10.1016/J.ENERGY.2015.12.064.
[60] Li Y, Du Y, Xu T, Wu H, Zhou X, Ling Z, et al. Optimization of thermal management system for Li-ion batteries using phase change material. Appl Therm Eng 2018;131:766–78. https://doi.org/10.1016/J.APPLTHERMALENG.2017.12.055.
[61] Safdari M, Ahmadi R, Sadeghzadeh S. Numerical investigation on PCM encapsulation shape used in the passive-active battery thermal management. Energy 2020;193:116840. https://doi.org/10.1016/j.energy.2019.116840.
[62] Yang Y, Chen L, Yang L, Du X. Numerical study of combined air and phase change cooling for lithium-ion battery during dynamic cycles. Int J Therm Sci 2021;165:106968. https://doi.org/10.1016/j.ijthermalsci.2021.106968.
[63] Kong D, Peng R, Ping P, Du J, Chen G, Wen J. A novel battery thermal management system coupling with PCM and optimized controllable liquid cooling for different ambient temperatures. Energy Convers Manag 2020;204:112280. https://doi.org/10.1016/j.enconman.2019.112280.
[64] Ping P, Zhang Y, Kong D, Du J. Investigation on battery thermal management system combining phase changed material and liquid cooling considering non-uniform heat generation of battery. J Energy Storage 2021;36:102448. https://doi.org/10.1016/j.est.2021.102448.
[65] Chen K, Hou J, Song M, Wang S, Wu W, Zhang Y. Design of battery thermal management system based on phase change material and heat pipe. Appl Therm Eng 2021;188:116665. https://doi.org/10.1016/j.applthermaleng.2021.116665.
[66] Abbas S, Ramadan Z, Park CW. Thermal performance analysis of compact-type simulative battery module with paraffin as phase-change material and flat plate heat pipe. Int J Heat Mass Transf 2021;173:121269. https://doi.org/10.1016/j.ijheatmasstransfer.2021.121269.
[67] Lin X-W, Zhou Z-F, Zhu X-G, Chen B, Zhu H, Ben N-Y, et al. Non-uniform thermal characteristics investigation of three-dimensional electrochemical-thermal coupled model for pouch lithium-ion battery. J Clean Prod 2023;417:137912. https://doi.org/10.1016/j.jclepro.2023.137912.
[68] Mahamud R, Park C. Spatial-resolution, lumped-capacitance thermal model for cylindrical Li-ion batteries under high Biot number conditions. Appl Math Model 2013;37:2787–801. https://doi.org/10.1016/j.apm.2012.06.023.
[69] Mama M, Solai E, Capurso T, Danlos A, Khelladi S. Comprehensive review of multi-scale Lithium-ion batteries modeling: From electro-chemical dynamics up to heat transfer in battery thermal management system. Energy Convers Manag 2025;325:119223. https://doi.org/10.1016/j.enconman.2024.119223.
[70] Lebrouhi BE, Lamrani B, Ouassaid M, Abd-Lefdil M, Maaroufi M, Kousksou T. Low-cost numerical lumped modelling of lithium-ion battery pack with phase change material and liquid cooling thermal management system. J Energy Storage 2022;54:105293. https://doi.org/10.1016/j.est.2022.105293.
[71] Smith K, Wang C-Y. Power and thermal characterization of a lithium-ion battery pack for hybrid-electric vehicles. J Power Sources 2006;160:662–73. https://doi.org/10.1016/j.jpowsour.2006.01.038.
[72] el Idi MM, Karkri M, Abdou tankari m, vincent s. Hybrid cooling based battery thermal management using composite phase change materials and forced convection. J Energy Storage 2021;41:102946. https://doi.org/10.1016/j.est.2021.102946.
[73] Jilte RD, Kumar R, Ahmadi MH, Chen L. Battery thermal management system employing phase change material with cell-to-cell air cooling. Appl Therm Eng 2019;161:114199. https://doi.org/10.1016/j.applthermaleng.2019.114199.
[74] Cicconi P, Kumar P, Varshney P. A support approach for the modular design of Li-ion batteries: A test case with PCM. J Energy Storage 2020;31:101684. https://doi.org/10.1016/j.est.2020.101684.
[75] Safdari M, Ahmadi R, Sadeghzadeh S. Numerical and experimental investigation on electric vehicles battery thermal management under New European Driving Cycle. Appl Energy 2022;315:119026. https://doi.org/10.1016/j.apenergy.2022.119026.
[76] Rubitherm GmbH n.d.